Small-Scale Spatial Variability of Radiant Energy for Snowmelt in a Mid-Latitude Sub-Alpine Forest

ALED ROWLANDS[1], JOHN POMEROY[1], JANET HARDY[2], DANNY MARKS[3], KELLY ELDER[4], AND RAE MELLOH[2]

ABSTRACT

This study assessed the spatial variability of downwelling longwave and shortwave radiation under dense and open evergreen canopies during the snowmelt period in the Rocky Mountains near Fraser, Colorado, USA. We compared their magnitudes and spatial distributions under cloudy and clear-sky conditions over a melting snowcover. Through the use of radiometer arrays, thermocouples, and a portable scanning thermal radiometer, a detailed picture of the spatial variability of radiant energy was gained. The variability of melt energy deriving from radiation on cloudy days was vastly reduced from that on sunny days. The sources of variability in melt energy were both long and shortwave but with fundamental differences.

INTRODUCTION

In open areas at small or 'sub-grid' scales the depletion of snow cover is often calculated using an initial statistical distribution of snow water equivalent and the assumption of constant melt energy applied to this distribution to determine the rate of areal snowmelt (e.g. Shook *et al.*, 1993; Donald *et al*., 1995; Brubaker and Menoes, 2001). Forested landscapes present an added level of complexity in which the energy available for snowmelt varies with canopy structural properties such as density (Davis *et al.*, 1997) and leaf area index (Pomeroy and Granger, 1997). Buttle and McDonnell (1987) noted that the rate of depletion of snow cover in forest stands was influenced by variation in snow accumulation or melt rate or some combination of the two. At sub-stand scales, absorption of shortwave radiation by trunks and branches and its redistribution as longwave energy to adjacent snow may affect the distribution of melt energy (Golding and Swanson, 1986; Verry *et al.*, 1983; Woo and Geisbrecht, 2000). Shallow snow near tree trunks may also have a lower albedo (Davis *et al.*, 1997) and leaf litter on the top of forest snowpacks lowers the albedo and increases net radiation to the snow in an irregular manner (Hardy *et al.*, 2000). The spatial distribution of energy applied to the surface has been shown to influence the rate of snow cover depletion and the areal mean snowmelt rate at small, sub-stand scales (Faria *et al.*, 2000). The melt energy distribution found by Faria *et al.* provided for greater snowmelt at locations with shallow snow. Pomeroy *et al.* (2001) showed that the small-scale spatial variation

[1]Institute of Geography and Earth Sciences, University of Wales, Aberystwyth, SY23 3DB UK
[2]US Army Cold Regions Research and Engineering Laboratory, 72 Lyme Road, Hanover, New Hampshire 03773-1290 USA
[3]USDA Agricultural Research Service, NW Watershed Research Center, 800 Park Avenue, Boise, Idaho 83712 USA
[4]Rocky Mountain Research Station, USDA Forest Service, 240 West Prospect Road, Fort Collins, CO 80526 USA

of sub-canopy energy within a white spruce stand in the Yukon Territory Canada was normally distributed with an overall coefficient of variation of 0.2 and temporally unstable. However, they were not able to ascribe the causes or sources of this instability. The purpose of this study was to examine the spatial variability of downwelling longwave and shortwave radiation under dense and open evergreen canopies and to compare their magnitudes and spatial distributions under cloudy and clear-sky conditions over a melting snowcover. Particular attention was paid to the dynamics of small-scale sources of sub-canopy longwave radiation.

METHODS

The experiments were conducted as part of NASA's Cold Land Processes Experiment (CLPX, http://www.nohrsc.nws.gov/~cline/clp.html) in a sub-alpine lodgepole pine forest (40°N, 105°W, 3066 m.a.s.l.) in the US Forest Service, Fraser Experimental Forest near Fraser, Colorado. The Fraser Experimental Forest is a long-term research facility of the Rocky Mountain Research Station and has been subject to stand management and snowmelt studies since the 1940's. Arrays of 20 shortwave and 4 longwave radiometers and 7 hypodermic type-E thermocouples were used to sample radiation fluxes and thermal conditions in a dense, relatively uniform mature pine stand and an adjacent open, highly heterogeneous stand. In the dense pine site, radiometers were located by selecting a random distance and angle from a central distribution point. In the open pine site, radiometer placement also considered proximity to tree trucks and placement in canopy gaps. Additionally, over 400 sub-canopy digital thermograms were collected using a specially cold-weather modified thermoelectric thermal infrared imaging radiometer, with a spectral range of 8 to 12 μm, and an absolute accuracy of 1.2°C and differential accuracy of 0.1°C. Each digital thermogram is 120 x 120 pixels. The instrument was mounted on a tripod and controlled from a linked laptop computer to obtain an image every 15 minutes from approximately 0730 until 1800h on three days. Separate tests with the imaging radiometer, narrow beam thermal infrared radiometers and hypodermic needle style thermocouples inserted into various natural surfaces onsite, confirmed that the imaging radiometer was operating well within accuracy specifications.

For the purposes of this paper, discussion is limited to a three-day period during the CLPX Intensive Observation Period 2 (IOP 2) from March 27th to 29th 2002 (Julian Days (JD) 86-88). The snowpack was isothermal and actively melting in this period and had become patchy in the open pine stand. The thermal infrared imaging radiometer was located in the same position in the dense stand during JD 86 and 87 but was positioned in the open pine stand during JD 88. Weather conditions for the three days are summarized in Table 1.

Date	Julian Day	Conditions	Minimum Air Temperature (°C)	Maximum Air Temperature (°C)	Position of scanning thermal radiometer
27/03/02	86	Overcast No precipitation	-6.8	3.8	Dense pine forest
28/03/02	87	Sunny – clear sky No precipitation	-3.1	6.5	Dense pine forest
29/03/02	88	Sunny – clear sky No precipitation	-7.0	6.2	Open pine forest

Table 1: Summary of the weather conditions and the position of the scanning thermal radiometer between JD 86 and 88, note air temperatures are sub-canopy, at 2-m above the snowpack.

RESULTS

Radiation Regime

Data were examined by comparing the incoming radiative fluxes above and beneath the canopy at the dense and open canopies on clear and cloudy days (Fig. 1). As expected, the sub-canopy radiative fluxes decreased from the incoming flux with increasing canopy density or leaf area, this effect was most evident under clear-sky conditions. Incoming above canopy shortwave radiation on JD 87 and 88 fits the classical shape indicating clear sky, direct radiation dominated conditions. On JD 86 variable cloud optical depth resulted in incoming fluxes that were substantially reduced compared to possible direct beam radiation, the degree of reduction varying to a large degree over the day. This represents classical cloudy, diffuse radiation dominated conditions. Attenuation of incoming radiation by the open stand canopy was much less on the cloudy day than on the clear days; this effect was less noticeable for the dense canopy.

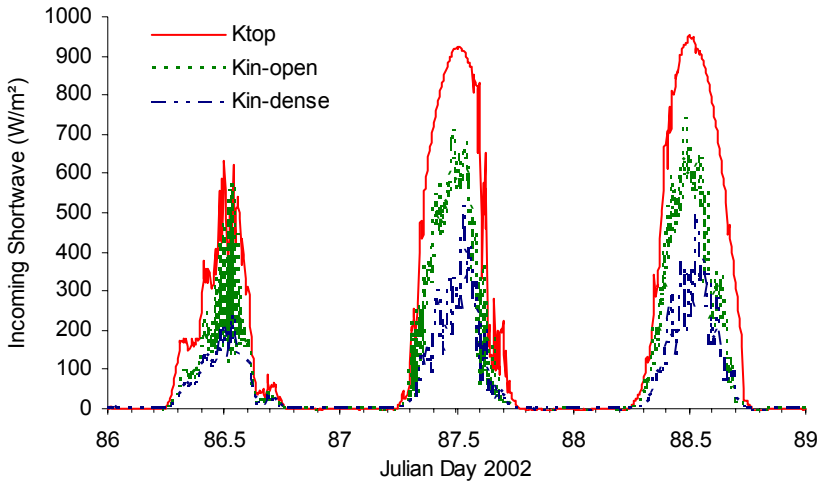

Figure 1: Incoming shortwave radiation measured above canopy and under open and dense pine canopies.

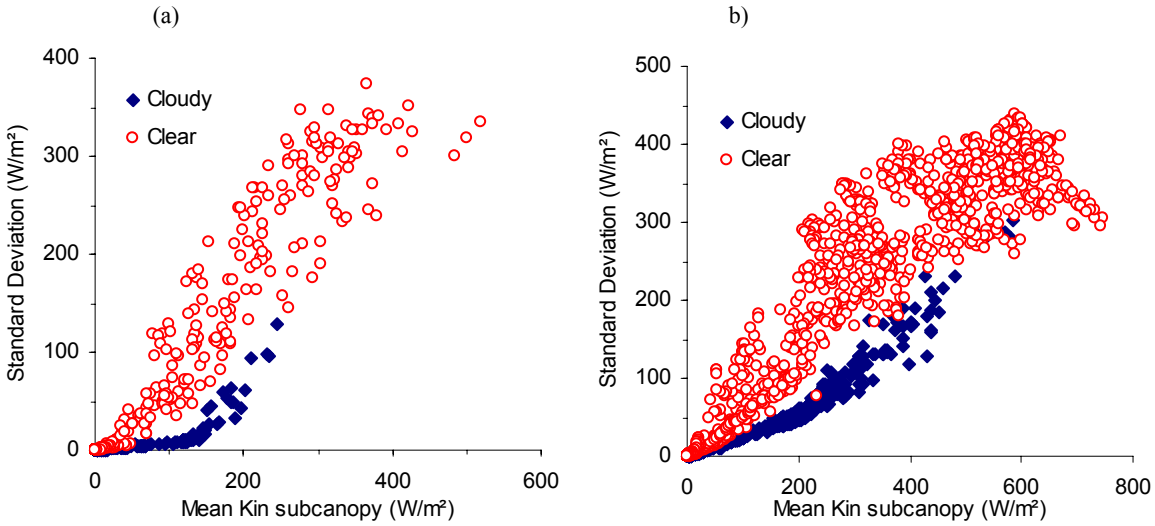

Figure 2: Standard deviation of shortwave incoming radiation in the (a) dense and (b) open forest. For (a) the sampling interval was 5 minutes and for (b) it was 1 minute.

Figure 2 shows the standard deviation for each measurement interval (one to five minutes) of the 10 incoming radiation measurements and the mean incoming shortwave radiation under each canopy type. There was less spatial variability of radiation on the cloudy day than on the clear day; the high degree of variability on the clear days suggests a coefficient of variation approximating 1. It should be noted that this degree of spatial variability is due to the short measurement intervals and averaging times (5 seconds) for these measurements. When radiation was summed and converted to MJ per day, the resulting coefficients of variation for daily shortwave radiation under the open canopy were 0.26 and 0.29 for clear and cloudy conditions respectively and 0.08 and 0.09 for the dense canopy, respectively. This suggests that the small-scale patterns of shortwave irradiances were not spatially stable over the day, though there was more structure to patterns in the open canopy as would be expected.

The pattern of incoming longwave radiation detected by radiometers under the dense and open forest canopies varies significantly over the study period. Minimal differences in downward fluxes were observed during cloudy conditions on JD 86. In contrast marked variations were observed during JD 87 and 88 reflecting the clear sky conditions. The sequence of magnitude of radiation flux with canopy density was reversed from that of shortwave with the largest downward longwave from the dense canopy and the smallest from the above canopy measurement.

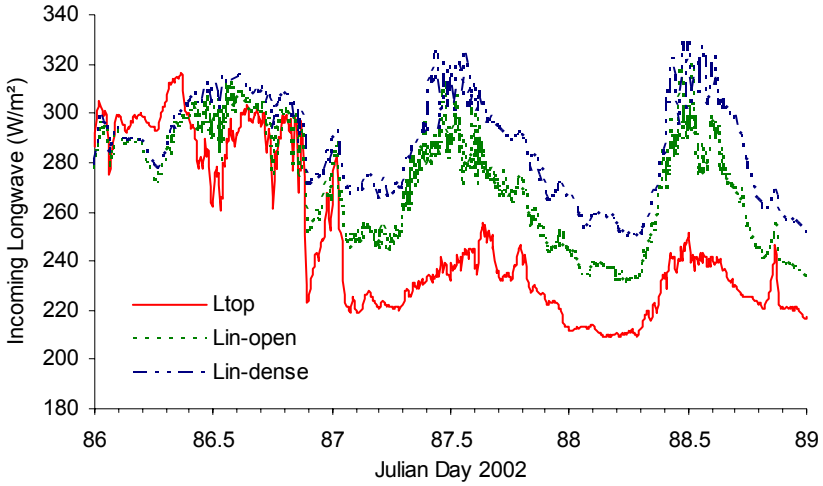

Figure 3: Incoming longwave radiation as measured above and beneath the canopies in the dense and open forest at Fraser.

Thermal Regime

The sub-canopy thermal regime monitored by hypodermic needle style thermocouples threaded into bark and stuck to needles indicates substantial differences between open and dense canopies with 'hot spots' such as lower trunks in the open canopy that were exposed to sun showing surface temperatures of up to 43°C (~560 W/m^2) on sunny days, whilst similar features in the dense canopy never warm above 15°C (~400 W/m^2) (Figure 4 a and b). In general, surface temperatures of trunk and needles in the dense canopy track closely together, whilst those in the open canopy are quite variable.

These surface temperatures may explain the differing thermal radiation regimes of the sites. Of interest is that features with large surface area to mass ratios such as needles seem to remain relatively cool despite their low albedo (in contrast to trunks), perhaps because of their relatively large surface area per unit mass to radiate thermal energy and undergo convective exchange with the cooler atmosphere.

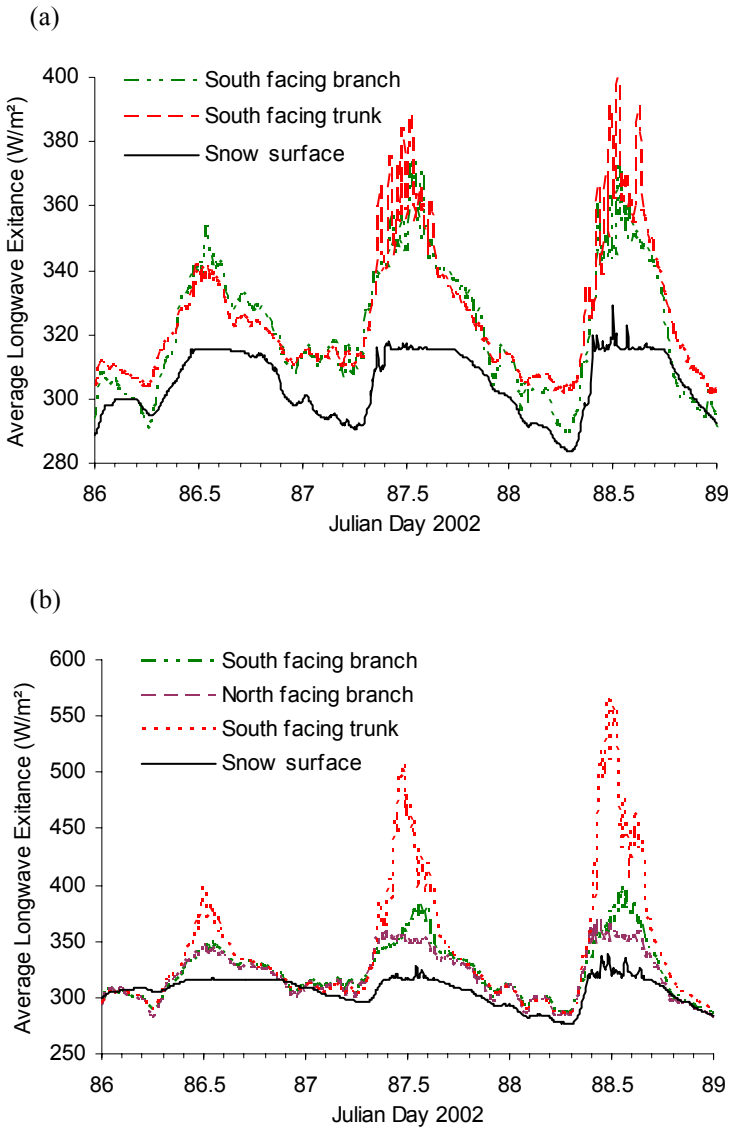

Figure 4: Temperature data, converted to W/m^2, obtained from thermocouples mounted in the (a) dense and (b) open forest.

Thermal Structure

The thermal structure of the sub-canopy environment can be elucidated more spectacularly and with greater spatial coverage using observations from the thermal infrared imaging radiometer (Figure 5). Images are presently undergoing calibration and analysis but a preliminary interpretation of thermal structure under the open canopy is instructive (Figure 5). Temperatures are shown as 'index temperatures', as at this point an emissivity of 1.0 was assigned to the whole image and actual emissivities will vary from this value. The area shown in Figure 5b was under intense irradiation in the morning of JD 88, when the index surface temperatures on the trunk reached near 20°C. Afternoon shading resulted in the index temperature distribution narrowing. Three elements of the scene were quantified. The ground elements (shrubs and snow) were quite restrained in their index temperature range despite similar radiative outputs. This reflects both differing emissivities and that the snow temperature was restricted by the 0°C limit upon which

further energy goes into phase change rather than an increase in temperature. The 'hot spots' evident on canopy elements play an important role in snow ablation as the visible light photograph shows a patch of bare ground surrounding one tree trunk and in fact melt proceeds from the trunks outwards in such environments (Faria *et al.*, 2000). The fixed location of trunks means that areas of high longwave exitance have a fixed spatial distribution, in contrast to the variable spatial distribution of shortwave over the course of a day.

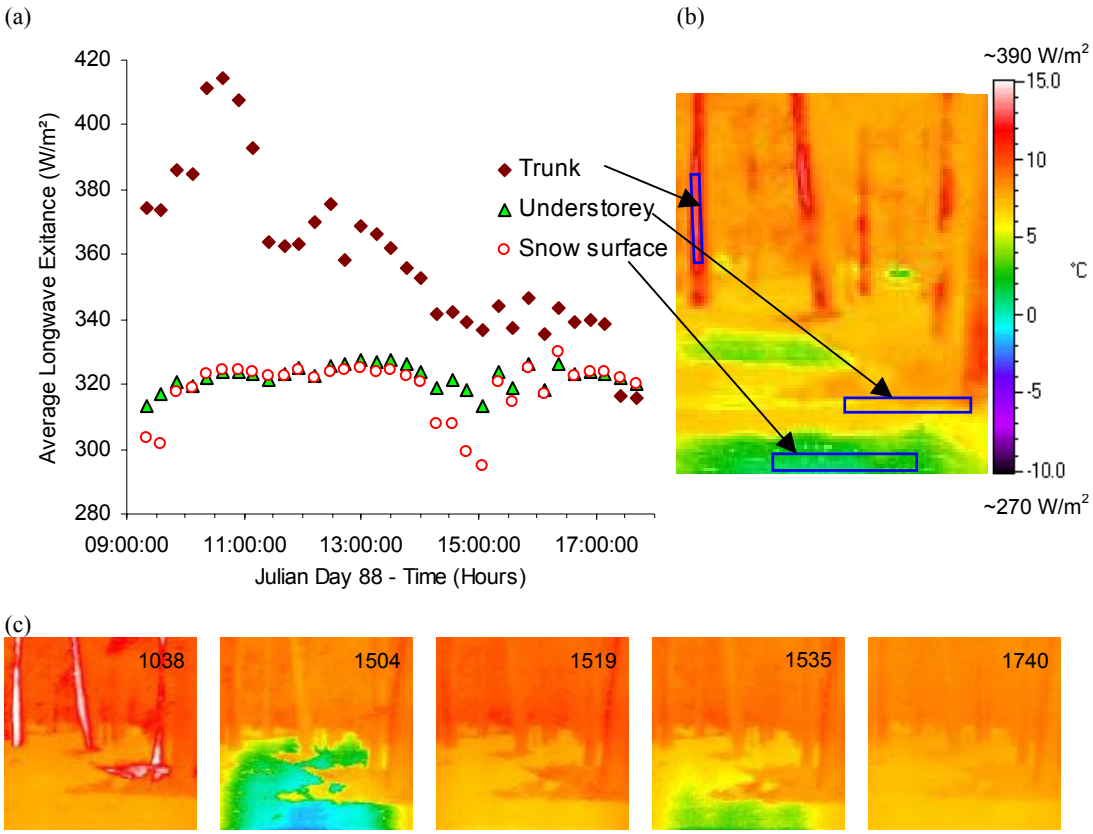

Figure 5: To illustrate the data obtained from the infrared imaging radiometer, a collection of graphs and images for JD 88 is presented. Three areas within the scene were identified (b) and mean temperature for each was calculated. The regions of interest focused on snow, understorey and trunk. Mean temperatures, converted to W/m^2, are shown in (a). The spatial variation in temperature throughout JD88 can be seen in the selection of thermographs (c). The thermographs are plotted as index temperatures (°C) presuming emissivity = 1.0 and for consistency are shown on the same temperature scale.

To quantify the spatial variation in the longwave radiation flux, thermograph scenes were divided into two zones (i) snow and (ii) above ground fraction (trunk and branches) to provide a spatial average of longwave exitance. The mean longwave radiation flux for both zones was computed for JD 86 – 88 (Figure 6). In contrast to cloudy JD 86, clear-sky JD 87 was characterized by marked fluctuations in the longwave flux of snow and the above ground component. The above ground component increased significantly during the day as the trunk, stem and branch temperatures increased with stomatal transpiration restricted. The longwave flux from snow increased during the morning but then reached a plateau in early afternoon because of the 0^{o}C restriction. Similar patterns were detected at higher temporal resolutions by thermocouples located on the snow surface and in a tree trunk at the same location (Fig. 4). The magnitude of the difference between minimum and maximum longwave flux during JD 88 (open canopy, clear-sky) was comparable to that observed in the dense forest on JD 87. The pattern of the flux during the

day was different, partially because of the more open nature of the forest. For example by the time measurements commenced on JD 88 the longwave flux from snow had already reached a plateau whereas during JD 87 the plateau was not attained until early afternoon.

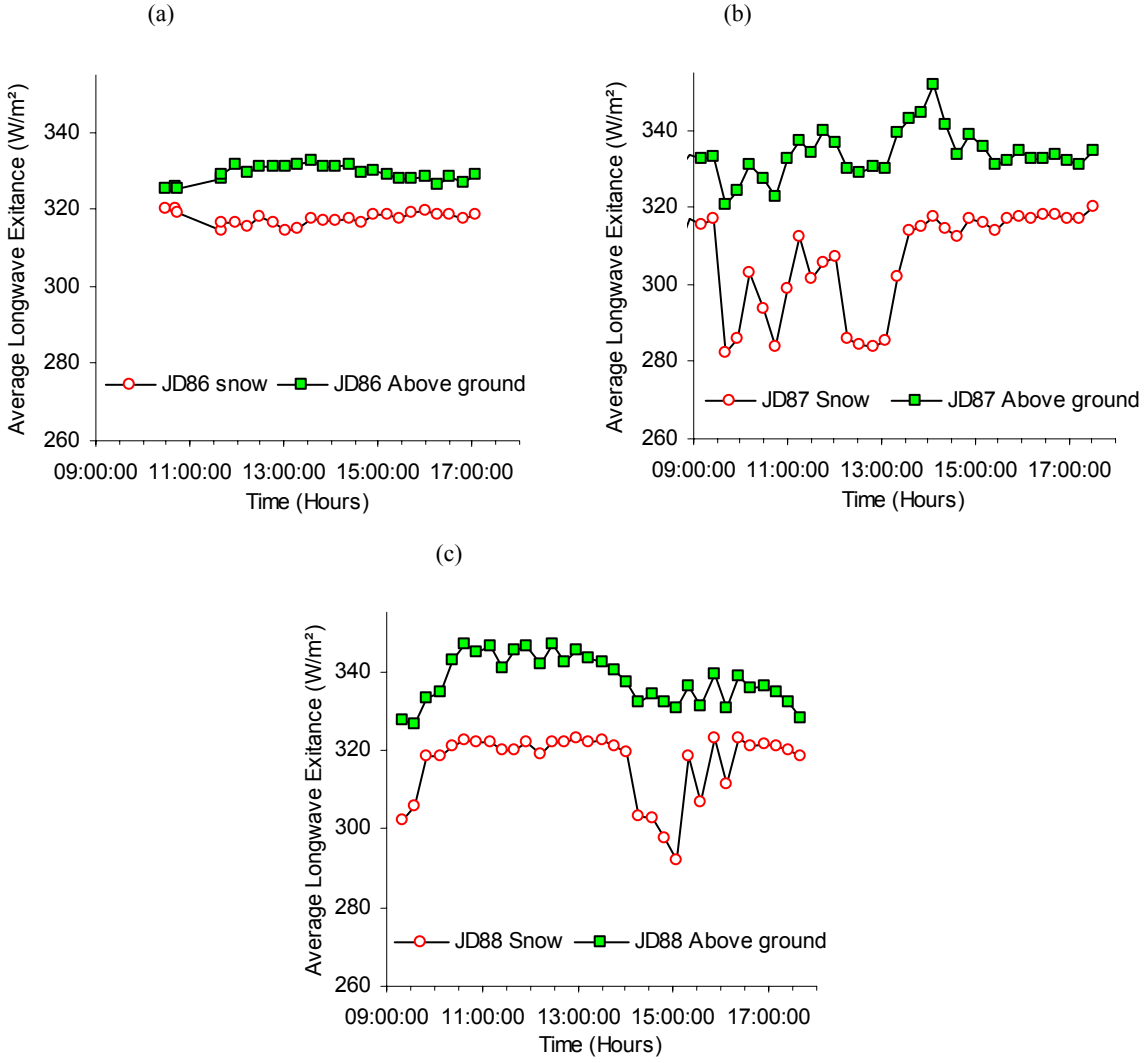

Figure 6: Data extracted from thermograph images obtained for (a) cloudy JD 86 (b) clear JD 87 and (c) clear JD 88. Images were divided into zones of snow and a combined category for trunks and branches. A mean temperature value was obtained for the two zones at 15-minute intervals.

The spatial variability of trunk and branch longwave exitance is illustrated as standard deviation of radiation compared to mean for short time intervals in Figure 7 a and b. Under overcast conditions the standard deviation of longwave canopy flux was minimal in comparison to that observed during clear sky conditions. The standard deviation was noticeably greater in the open forest. In most cases the high standard deviation values represented measurements taken in late afternoon. While the standard deviations for relatively instantaneous longwave spatial distributions were quite low compared to that of incoming shortwave radiation, the distribution of longwave was spatially fixed and persisted until after sunset as it was controlled by the geometry of trunk, stem and branch locations. The coefficient of variations of longwave exitance from the image, averaged on a daily basis for the images were 0.020 and 0.012 for open and dense pine respectively on the clear day with the value decreasing to 0.006 for the dense pine on the cloudy

day. This degree of daily spatial variation was on the whole smaller than that for shortwave irradiation on the same days, though these statistics were not strictly compatible.

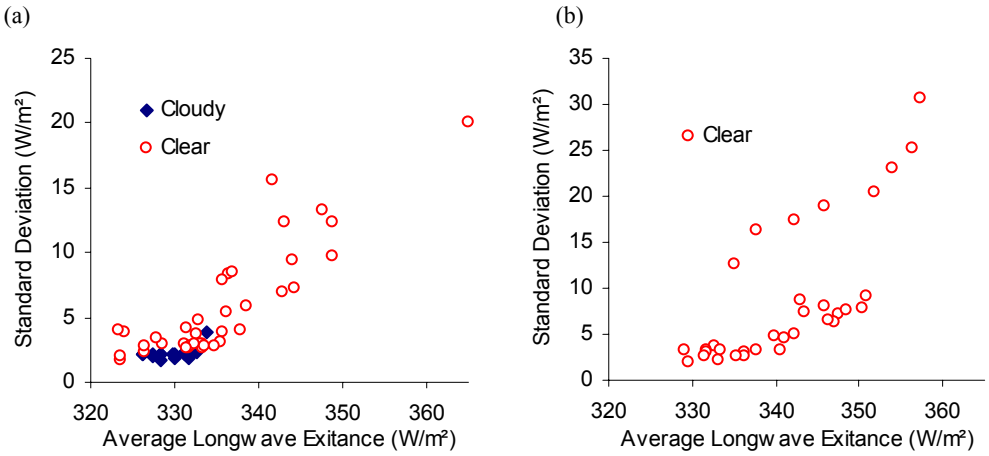

Figure 7: Standard deviation values of longwave canopy exitance plotted against average longwave exitance from trunks and branches in the (a) dense and (b) open forest.

CONCLUSIONS

The scanning thermal radiometer is a very effective tool for visualizing and measuring the spatial distribution of longwave flux. Results from the instrument correlated well with surface temperature measurements when expressed as longwave radiative fluxes. The variability of melt energy deriving from radiation on cloudy days was vastly reduced from that on sunny days. The source of variability in melt energy were both long and shortwave but with fundamental differences. Incoming sub-canopy shortwave energy had a wide spatial distribution that changed continuously over the day with solar position with respect to the canopy scattering elements. The variability of this distribution for short time intervals was similar for open and dense canopies despite much less insolation in dense canopies. However when daily insolation was considered, the open canopy had a much more spatially variable irradiation than the dense canopy, because the larger gaps in the open canopy imposed a more consistent spatial structure on incoming shortwave. The spatially dynamical nature of this distribution of energy for dense canopies suggested that simple mean representations were sufficient for melt energy modeling. Spatial longwave radiation distributions for short time intervals were relatively narrow compared to shortwave. The spatial distribution of longwave was relatively fixed and was attributed to positions of trunks and low-lying branches. The range of surface temperatures causing this distribution changed with insolation and resulted in much greater variance on sunny days than on cloudy days. The variability of longwave radiance was also much greater in open than in dense canopies. When daily radiation inputs were considered however, the spatial variability of sub-canopy shortwave was much greater than that of longwave flux and appears to exert a greater role in controlling the spatial distribution of downwelling radiant energy under forest canopies.

ACKNOWLEDGEMENTS

The financial support of the US Army Corps of Engineers, Cold Regions Research and Engineering Laboratory is greatly appreciated. The support, planning and encouragement of Don Cline, US National Weather Service, Bert Davis, US Army CRREL and others from NASA's Cold Land Processes Mission planning group for this and the overall CLPX study was essential in supporting this particular experiment and a much wider range of measurements at this time. The

Fraser Experimental Forest facilities are maintained and operated by Manuel Martinez of the Rocky Mountain Research Station, Fort Collins who is warmly thanked. Finally the infrared and surface temperature measurement equipment used for much of this study was provided by a grant to the Institute of Geography and Earth Sciences, University of Wales, Aberystwyth from the Strategic Research Investment Fund through the Welsh Assembly Government, Wales.

REFERENCES

Brubaker, K.L. and M Menoes, 2001. A technique to estimate snow depletion curves from time-series data using the beta distribution. *Proceedings of the Eastern Snow Conference*, **58**, 343-346.

Buttle, J.M. and J.J. McDonnel, 1987. Modeling the areal depletion of snowcover in a forested catchment. *Journal of Hydrology*, **90**, 43-60.

Davis, R. E., Hardy, J. P., Ni, W., Woodcock, C., McKenzie, J. C., Jordan, R. and Li, X. 1997. Variation of snow cover ablation in the boreal forest: A sensitivity study on the effects of conifer canopy. *Journal of Geophysical Research*, **102**, 29389-29395.

Donald, J.R., E. D. Soulis, N. Kouwen and A. Pietroniro 1995. A land cover-based snow cover representation for distributed hydrological models. *Water Resources Research*, **31**(4), 995-1009.

Faria, D.A., Pomeroy, J.W. and R.L.H. Essery, 2000. Effect of covariance between ablation and snow water equivalent on depletion of snow-covered area in a forest. *Hydrological Processes*, **14**, 2683-2695.

Golding, D. L. and Swanson, R. H. 1986. Snow distribution patterns in clearings and adjacent forest. *Water Resources Research*, **22**, 1931-1940.

Hardy, J.P., Melloh, R., Robinson, P. and R. Jordan, 2000. Incorporating effects of forest litter in a snow process model. *Hydrological Processes*, **14**, 3227-3237.

Pomeroy, J.W. and R.J. Granger, 1997. Sustainability of the western Canadian boreal forest under changing hydrological conditions - I- snow accumulation and ablation. In (eds. D. Rosjberg, N. Boutayeb, A. Gustard, Z. Kundzewicz and P Rasmussen) Sustainability of Water Resources under Increasing Uncertainty. IAHS Publ No. 240. IAHS Press, Wallingford, UK. 237-242.

Pomeroy, J. W., Gray, D. M., Shook, K. R., Toth, B., Essery, R. L. H., Pietroniro, A. and Hedstrom, N. 1998. An evaluation of snow accumulation and ablation processes for land surface modeling. *Hydrological Processes*, **12**, 2339-2367.

Pomeroy, J.W., Hanson, S. and Faria, D.A. (2001) Small-scale Variation in Snowmelt Energy in a Boreal Forest: an Additional Factor Controlling Depletion of Snow Cover? *Proceedings of the Eastern Snow Conference,* **58**, 85-96.

Shook, K., J.W. Pomeroy, D.M. Gray. 1993. Temporal variation in snow-covered area during melt in Prairie and Alpine environments. *Nordic Hydrology*, **24**, 183-198.

Verry, E. S., Lewis, J. R. and Brooks, K. N. 1983. Aspen clear cutting increases snowmelt and storm flow peaks in north central Minnesota. *Water Resources Bulletin*, **19**, 59-67.

Woo, M. and M.A. Giebrecht, 2000. Simulation of snowmelt in a subarctic spruce woodland: 1. Tree model. *Water Resources Research*, **36**(8), 2275-2285.